

Boltzmann-Uehling-Uhlenbeck and relaxation time methods: A comparison

H. S. Köhler*

Nuclear Science Division, Lawrence Berkeley Laboratory, University of California, Berkeley, Berkeley, California 94720

W. Bauer

National Superconducting Cyclotron Laboratory and Physics Department, Michigan State University, East Lansing, Michigan 48824

(Received 9 May 1989)

The Boltzmann-Uehling-Uhlenbeck and relaxation time methods are compared numerically for collisions between two ^{16}O nuclei. Phase-space trajectories and double differential cross sections for nucleon emission are compared. Results are practically identical although the relaxation time method exhibits a slightly higher degree of stopping power.

I. INTRODUCTION

Several theoretical models have been developed for calculating large amplitude nuclear dynamics. The first successful model was the time-dependent Hartree-Fock (TDHF) approximation. It has been applied quite extensively to the study of low-energy heavy-ion collisions.¹ In its standard form this is a microscopic theory for nucleons without nucleonic internal degrees of freedom. Here two-body excitations due to nucleon-nucleon collisions are neglected. The nucleons are assumed to interact with some effective interaction which could be the Brueckner reaction matrix but in most applications some simple version of "Skyrme-type" force is used to generate the mean field. The TDHF approximation is analogous to neglecting the absorptive (imaginary) part of the optical model potential for nucleon-nucleus (or nucleus-nucleus) scattering while retaining only the real part. The imaginary part is essentially zero at very low energy but increases with bombarding energy. This is a consequence of the Fermi statistics for the nucleons. Absorption increases with energy as available phase space opens up, allowing for two-body excitations and the imaginary part of the optical potential can no longer be neglected. TDHF has to be improved in a similar fashion as the energy of the system, i.e., bombarding energy, increases.

The classical correspondence to TDHF is the Vlasov equation.² This equation is, on the other hand, derived from the original Boltzmann equation by neglecting two-body excitations. The corresponding improvement of TDHF is therefore implemented by a quantum (Q) version of the Boltzmann equation, such as derived by Kadanoff and Baym³ (see also Danielewicz⁴). This contains in addition to the mean field (defined as in TDHF), a quantum collision operator. The Q collision operator reduces in the classical limit to the Boltzmann collision term. For Fermions this should be replaced by the so-called Uehling-Uhlenbeck⁵ (Nordheim) collision term, that we refer to as UU. In the time-dependent Hartree-Fock relaxation-time (TDHFRX) model introduced by one of us,⁶ this collision term is approximated by the relaxation-time (RX) method. This approximation has been tested numerically against both the UU and the Q collision operator for infinite nuclear matter.^{4,7} The

agreement with the latter is actually somewhat better. The difference between the UU and Q calculations is that the Q (and RX) model puts nucleons up in high momentum states after fewer collisions than do the UU calculations. This is the result of the conservation of energy in individual collisions imposed in UU, while Q and RX calculations only impose an averaged energy conservation. One may argue that the difference should decrease with total energy as the system then should become more classical. The final distribution is for an infinite system in all three cases (Q , RX, and UU) a Fermi distribution defined by conservation of energy, particle number, and total momentum. The difference between the three may, therefore, not be observed in studying nuclear matter, but one can expect differences to be found in finite systems where different degrees of equilibration may be obtained.

By taking the semiclassical limit of both the mean-field operator and of the collision term, one obtains the Boltzmann- (or Vlasov-) Uehling-Uhlenbeck (BUU or VUU) model. Several computational methods have been designed for solving these equations. We shall apply here the method for BUU which was developed by one of us, and which was shown to correctly reproduce the experimental particle emission cross sections for intermediate-energy heavy-ion reactions.⁸

The BUU and TDHFRX models, although rather different in appearance, are nevertheless very similar in physical content. Both include a mean-field and a two-body collision term, although in different approximations as discussed above.

It is of interest to make a direct numerical comparison between the two models. Of course, to make such a comparison meaningful one has to use the same interaction for deriving the mean field, and the two-body collisions would also have to be the same. Although in principle this can be achieved, the comparison would still be somewhat obscured by the very different methods of solution.

In this paper we shall limit ourselves to a comparison between the collision terms. We accomplish this by replacing the collision term in BUU by the RX collision term. We shall find that the original BUU results are well reproduced after this replacement. A comparison will show that, in practice, these two methods lead to quite similar results.

II. VLASOV WITH RELAXATION TERM

The replacement of the UU collision term with a RX collision term, although in principle straightforward, is in practice not quite obvious. The reason is the large difference between the two computer programs solving the BUU and TDHFRX equations. Therefore, before showing how the replacement is accomplished, we briefly highlight the important steps in these two programs.

The TDHFRX program time develops a density-matrix $\rho(\mathbf{R}, \mathbf{x}, t)$. At time $t=0$ this is calculated from the Hartree-Fock solutions for the two colliding nuclei

$$\rho(\mathbf{R}, \mathbf{x}, 0) = \sum_{i=1}^{\infty} n_i \Psi_i^*(\mathbf{R} + \frac{1}{2}\mathbf{x}) \Psi_i(\mathbf{R} - \frac{1}{2}\mathbf{x}). \quad (1)$$

After boosting, propagation under the influence of the mean field is obtained by time developing this density matrix by the TDHF equation

$$i\hbar \frac{d}{dt} \rho(\mathbf{R}, \mathbf{x}, t) + \frac{\hbar^2}{2m} \nabla_{\mathbf{R}} \cdot \nabla_{\mathbf{x}} \rho(\mathbf{R}, \mathbf{x}, t) + [U(\mathbf{R} + \frac{1}{2}\mathbf{x}, t) - U(\mathbf{R} - \frac{1}{2}\mathbf{x}, t)] \rho(\mathbf{R}, \mathbf{x}, t) = 0. \quad (2)$$

In the relaxation-time method, the redistribution of particles in momentum space due to the two-body collisions is calculated from

$$\left[\frac{d\rho(\mathbf{R}, \mathbf{x}, t)}{dt} \right]_c = - \frac{\rho(\mathbf{R}, \mathbf{x}, t) - \rho_0(\mathbf{R}, \mathbf{x}, t)}{\tau(\mathbf{R}, t)}. \quad (3)$$

$$\left[\frac{df(\mathbf{R}, \mathbf{p}, t)}{dt} \right]_c = \frac{g}{2\pi^3 m^2} \int d^3 q_1 d^3 q_2 d^3 q_2' \delta \left[\frac{1}{2m} (p^2 + q_2^2 - q_1^2 - q_2'^2) \right] \delta^3(\mathbf{p} + \mathbf{q}_2 - \mathbf{q}_1 - \mathbf{q}_2') \frac{d\sigma}{d\Omega} \times \{ \bar{f}(\mathbf{r}, \mathbf{q}_1, t) \bar{f}(\mathbf{r}, \mathbf{q}_2, t) [1 - \bar{f}(\mathbf{r}, \mathbf{p}, t)] [1 - \bar{f}(\mathbf{r}, \mathbf{q}_2, t)] - \bar{f}(\mathbf{r}, \mathbf{p}, t) \bar{f}(\mathbf{r}, \mathbf{q}_2, t) [1 - \bar{f}(\mathbf{r}, \mathbf{q}_1, t)] [1 - \bar{f}(\mathbf{r}, \mathbf{q}_2', t)] \}. \quad (5)$$

In the relaxation time method, on the other hand, the redistribution is accomplished by applying Eq. (3), i.e., by the substitution of the distribution obtained from mean-field propagation $f(\mathbf{R}, \mathbf{p}, t)$ at each time step by

$$f_{\text{rlx}}(\mathbf{R}, \mathbf{p}, t) = f_0(\mathbf{R}, \mathbf{p}, t) + [f(\mathbf{R}, \mathbf{p}, t) - f_0(\mathbf{R}, \mathbf{p}, t)] \exp \frac{-\Delta t}{\tau(\mathbf{R}, t)}. \quad (6)$$

Here Δt is the time step and

$$f_0(\mathbf{R}, \mathbf{p}, t) = \left[1 + \exp \frac{[\mathbf{p} - \bar{\mathbf{p}}(\mathbf{R}, t)]^2 / 2M - \mu(\mathbf{R}, t)}{T(\mathbf{R}, t)} \right]^{-1} \quad (7)$$

is the local Fermi distribution boosted with the local average momentum $\bar{\mathbf{p}}(\mathbf{R}, t)$. It is simply related to $\rho_0(\mathbf{R}, \mathbf{x})$ by the Fourier transformation [Eq. (4)].

The model resulting from combining the Vlasov equation with the relaxation time method will be referred to

Here, ρ_0 is the relaxed Fermi distribution that depends on \mathbf{R} and t through the space- and time-dependent temperatures and chemical potentials. The relaxation time τ also depends on \mathbf{R} and t through the densities and temperatures [see Eqs. (11) and (12)].

The Fourier transform of $\rho(\mathbf{R}, \mathbf{x}, t)$ with respect to \mathbf{x} is the Wigner function $W(\mathbf{R}, \mathbf{p}, t)$

$$W(\mathbf{R}, \mathbf{p}, t) = (2\pi)^{-3} \int \exp(i\mathbf{p} \cdot \mathbf{x}) \rho(\mathbf{R}, \mathbf{x}, t) d\mathbf{x}. \quad (4)$$

The classical correspondence of this function is the distribution function $f(\mathbf{R}, \mathbf{p}, t)$. The function f is positive definite while W also can be negative. The magnitude of the negative values are always very small, however, giving credence to the suggestion that the collisions are governed essentially by classical mechanics.⁹ The small values at time $t=0$ are a confirmation of the validity of the Thomas-Fermi method for ground-state nuclei.

In BUU a distribution function is obtained through averaging over an ensemble of systems which are time developed in parallel. At time $t=0$ the ensemble is prepared by labeling all "test particles" (equal to the number of "real" particles times the number of systems in the ensemble) and randomly placing them inside a predetermined volume in phase space. Each test particle is assigned a coordinate and a momentum. When time stepping through the mean field, these coordinates and momenta are changed by Newtonian mechanics.

The two-body collisions are included in BUU by allowing particles to collide with an N - N crosssection and with the outgoing particles obeying the Pauli principle

as the VRX model and this model will now be described. The two-body collision term has the effect of repopulating the particles in momentum (but not coordinate) space. The calculation of this repopulation is, therefore, done (at each time step) separately within each coordinate bin (of size 1 fm^3). To calculate the Fermi distribution at each point \mathbf{R} from Eq. (7) we need the temperature $T(\mathbf{R}, t)$, the chemical potential $\mu(\mathbf{R}, t)$, and the average momentum $\bar{\mathbf{p}}(\mathbf{R}, t)$. The latter is obtained simply from averaging the momenta of all particles within a coordinate bin. The temperature and the chemical potential are obtained from the particle and energy densities but this requires some discussion. The distribution $f(\mathbf{R}, \mathbf{p}, t)$ is not a thermalized distribution (locally or globally) and a temperature can, therefore, not be assigned to this distribution. The temperature to be defined is rather the temperature of this distribution if it were allowed to thermalize locally. This thermalization takes place by particle, total momentum, and energy-conserving two-body collisions. The two-body potential from which the mean field is calculated is in the present work assumed to be local; i.e., momentum independent.

(A momentum dependence would lead to formally simple modifications of what follows.) The potential energy is consequently independent of the distribution in momentum space. Therefore only kinetic energies have to be considered here. It follows that the particle density, average momentum, and kinetic energy (calculated from zero, first, and second moments in \mathbf{p}) of the Fermi distribution $f_0(\mathbf{R}, \mathbf{p}, t)$ is the same as that of $f(\mathbf{R}, \mathbf{p}, t)$ at each coordinate \mathbf{R} . These five invariants of the two-body collisions suffice, in fact, to define $f_0(\mathbf{R}, \mathbf{p}, t)$. The temperatures $T(\mathbf{R}, t)$ and chemical potentials $\mu(\mathbf{R}, t)$ are obtained from the moments by interpolation in an initially calculated table of zero and second moments of $f_0(\mathbf{p})$ as functions of the temperature and chemical potential. For low temperatures ($T \leq 5$ MeV) and to start the interpolation, the well-known expansion is used, i.e.,

$$T(\mathbf{R}, t) = \left[6[e(\mathbf{R}, t) - e_0(\mathbf{R}, t)]k_F^{-1} \frac{\hbar^2}{2M} \right]^{1/2}, \quad (8)$$

$$\mu(\mathbf{R}, t) = e_F(\mathbf{R}, t) - \frac{\pi^2}{12} T(\mathbf{R}, t)^2 / e_F(\mathbf{R}, t). \quad (9)$$

Here $e(\mathbf{R}, t)$ is the kinetic-energy density (second moment) and

$$e_0(\mathbf{R}, t) = \frac{3}{10} \frac{\hbar^2}{2M} k_F^2(\mathbf{R}, t) \rho(\mathbf{R}, t) \quad (10)$$

is the kinetic-energy density of ground-state nuclear matter at density $\rho(\mathbf{R}, t)$ while $k_F(\mathbf{R}, t)$ and $e_F(\mathbf{R}, t)$ are the corresponding Fermi momentum and energy, respectively.

The relaxation time is a function of temperature and density and on the mode of deformation with τ_κ (heat-conductivity mode) and τ_η (viscosity mode) given by¹⁰

$$\tau_\kappa = 1.033 T^{-2} q^{0.4} (1 + 0.1 T/q) + \frac{0.19 T^{1/2}}{q (1 + 160 T^{-2})}, \quad (11)$$

$$\tau_\eta = 2.833 T^{-2} q^{0.333} (1 + 0.04 T/q) + \frac{0.127 T^{1/2}}{q (1 + 160 T^{-2})}, \quad (12)$$

where $q = \rho(\mathbf{R}, t) / \rho_0$ with $\rho_0 = 0.145 \text{ fm}^{-3}$ being the normal (saturation) nuclear matter density. $T = T(\mathbf{R}, t)$ is the temperature as determined above in units of MeV. The distinction between temperatures to be used in the density-matrix and relaxation time calculations is neglected here.⁶ We find that $\tau_\eta / \tau_\kappa \sim 3$ for low temperatures. For temperatures below ~ 7 MeV, the relaxation time is quite large however and two-body collisions can be ignored. It decreases rapidly with temperature but the above ratio simultaneously decreases to ~ 1 at 20 MeV, which is a typical temperature at the bombarding energy considered here. We therefore neglect the dependence on mode of deformation and take the average value of the two relaxation times.

As mentioned, each test particle is initially labeled and the time evolution tracks the coordinate and momentum of each test particle. We can therefore easily find the la-

bels and total number of all the test particles within a given momentum bin. The two-body collisions will change this by a number proportional to $f_{\text{rx}}(\mathbf{p}) - f(\mathbf{p})$. This number may be positive or negative. If the total of this number is negative within a particular momentum bin, particles will scatter out of that bin. We refer to this number as $N_-(i)$ where i labels the bin. Likewise $N_+(j)$ indicates the number of particles that scatter into bin j . The repopulation of particles is now made by removing particles, one at a time, from the bin where $N_-(i)$ has a maximum and moving it to the bin where $N_+(j)$ is a maximum. The momentum of the nucleon in the new bin was chosen at random within the bin to which the nucleon was moved. In most calculations, the size of each bin was taken to be about $(0.5 \text{ fm}^{-1})^3$ with about 20^3 bins totally for each coordinate \mathbf{R} .

III. COMPARISON

For the comparison between the BUU and VRX methods defined above we studied collisions between ^{16}O nuclei in the center-of-mass (c.m.) systems with an energy corresponding to a laboratory energy of 80 MeV/nucleon.

Figure 1 shows the trajectories of the two colliding nu-

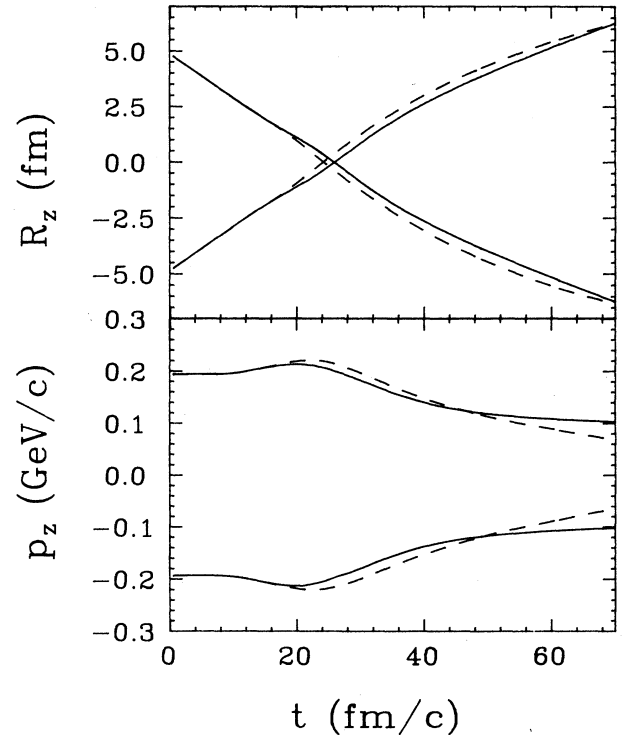


FIG. 1. Phase-space trajectories (upper part of figure is coordinate and lower is momentum) for a head-on collision between two ^{16}O nuclei at 80 MeV/nucleon. The full lines are BUU results while dashed lines show relaxation time results. Displayed are the longitudinal c.m. coordinates and momenta for target and projectile.

clei in coordinate and momentum space for a head-on collision. The coordinate is the center of mass and the momentum is the average momentum for each nucleus. At $t=0$ the two nuclei are located at $+5$ and -5 fm, respectively, and with momenta per nucleon of $+0.2$ and -0.2 GeV/c. The solid lines show the BUU trajectories while the dashed are the VRX results. The nuclei are initially not interacting and free space trajectories are seen before $t=20$ fm/c. There is in both cases (BUU and VRX) a slight increase in average momentum as the nuclei start touching and experience attraction due to the attractive component of the mean field of the other nucleus. The VRX momenta are subsequently about 10% higher than the ones obtained from BUU, and this situation reverses later in the collision. This is an indication that VRX exhibits a higher degree of nuclear stopping power than BUU. Concentrating on the final momenta at $t=65$ fm/c, the dissipation of momentum appears to be somewhat larger in the VRX case.

Figure 2 shows the corresponding trajectories for an impact parameter of 5 fm. The agreement between the two models is in this case almost perfect. This is hardly surprising. For peripheral collisions the influence of the nucleon-nucleon collisions on the overall reaction trajectories should be marginal; and the motion of the nucleons in the nuclear mean field is in both approaches governed by the same equations.

In Fig. 3 we show the energy dependence of particle

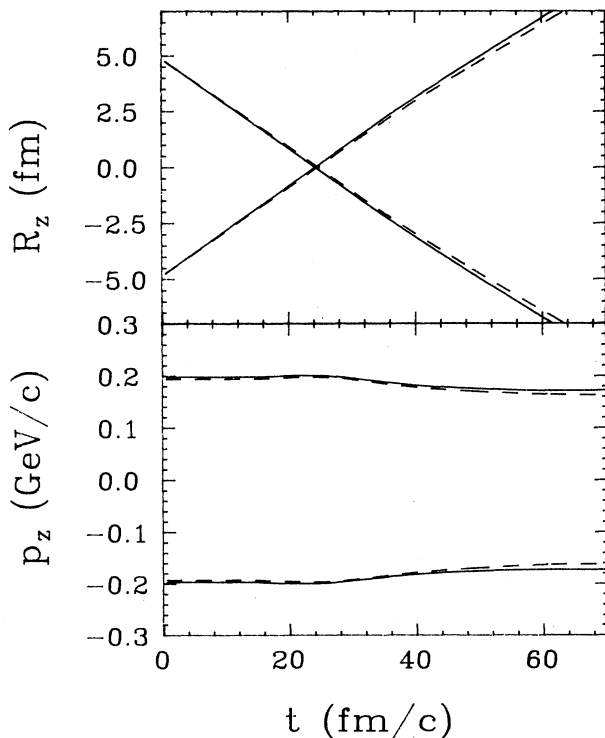


FIG. 2. Phase-space trajectories (upper part of figure is coordinate and lower is momentum) for a collision between two ^{16}O nuclei at 80 MeV/nucleon and at an impact parameter of 5 fm. The full lines are BUU results while dashed lines show relaxation-time results.

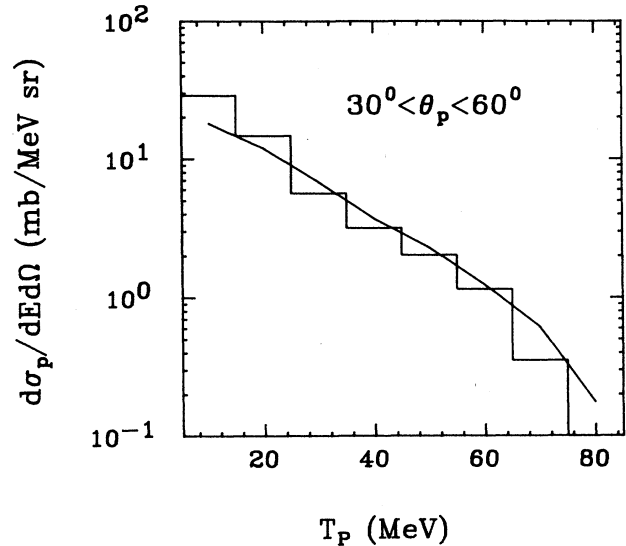


FIG. 3. Double differential cross sections for the emission of nucleons from the head-on collision of two ^{16}O nuclei at 80 MeV/nucleon. The histogram shows the BUU result while the full line is the relaxation result.

emission. Double differential cross sections are shown as a function of energy for particles emitted between 30° and 60° . The histogram is the BUU and the full line is the VRX result. The agreement is obvious. In both cases we obtain the same answer within the statistical error bars due to the finite number of test particles used in the calculation. Only in the lowest energy bin do we have some disagreement. This is probably due to the fact that in the VRX approach the outgoing projectile and target remnants have less kinetic energy, and thus tend to reabsorb more nucleons with small kinetic energies. However, the extracted slope parameters ("temperature") are the same in both cases.

In Fig. 4 we investigate the angular dependence of the proton emission cross section as calculated in both models. Again, the histogram is the result of the BUU calculation and the full line represents the VRX model. Here we display the energy integrated angular distributions which were grouped in bins of width 30° . It is clear that in this procedure the angular distributions will be dominated by the low-energy protons. However, we have verified that the double differential angular distributions have a similar shape to the one obtained in Fig. 4. Due to the fact that VRX emits slightly less nucleons into the low-energy bins, we had to scale its results up by a factor of 1.5 in Fig. 4 for the sake of comparison.

From Fig. 4 we can first observe that, as required, in both approaches we obtain a forward-backward symmetry of the angular distribution. The small deviations which are visible in the VRX method are due to the statistical fluctuations due to the finite number of test particles used. The ratio of the cross section at 90° to the cross section at 0° or 180° is a measure for the anisotropy in the final state momentum space occupancy. The values obtained for this ratio are $\sigma_p(90^\circ)/$

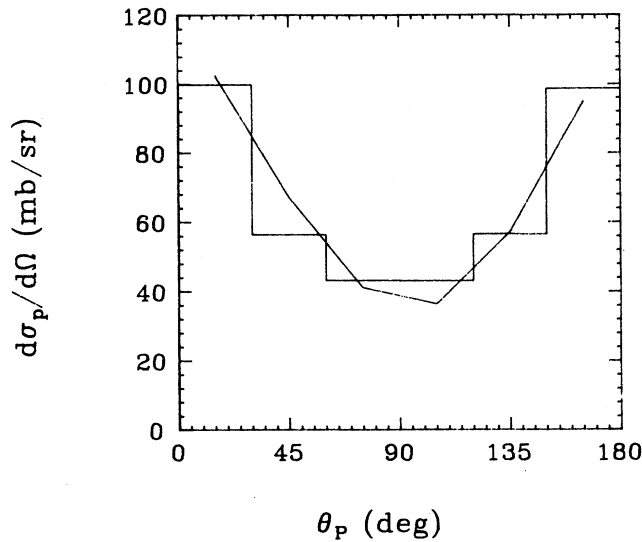


FIG. 4. Angular dependence of the particle emission cross sections in the BUU (histogram) and VRX (full line) models. For purposes of comparison, the VRX results are scaled up by a factor of 1.5.

$\sigma_p(0^\circ) = 0.43$ for BUU and $\sigma_p(90^\circ)/\sigma_p(0^\circ) = 0.39$ for VRX. Both calculations, therefore, show similar degrees of thermalization. For comparison, a completely thermalized and therefore isotropic source would have $\sigma_p(90^\circ)/\sigma_p(0^\circ) = 1$.

IV. COMMENTS AND CONCLUSIONS

A new model for heavy-ion collisions has been tested. It replaces the UU collision term with a relaxation term and is coined the VRX model. We find that the two models VRX and BUU are in very good agreement for the cases we tested. The agreement implies that the relaxation time model well reproduces the UU collisions. This is not altogether unexpected because both calculations are based on the same input as far as two-body collisions are concerned. In the BUU model this is done explicitly. In the VRX model, meanwhile, it is done indirectly. The UU collision term results in a thermalization, i.e., relaxation, of the distribution towards thermal equilibrium. This relaxation is calculated in nuclear matter and is fitted with a relaxation time that is a function of density and, more importantly, of final temperature which stems from the effect of Pauli blocking. The difference between the models is, therefore, more in method of calculation than in physical content. Nevertheless, it is very satisfying to find the agreement to be so good, because the methods of calculation are very different and it gives us increased confidence in these methods. From a practical point of view the VRX model has a slight advantage, as the computer program is about a factor of 2 faster.

This work was supported in part by the National Science Foundation, under Grant Nos. PHY86-04602 and PHY87-14432, and the U. S. Department of Energy under Contract No. DE-AC03-76SF00098.

*Permanent address: Physics Department, University of Arizona, Tucson, AZ 85721.

¹K. T. R. Davies, K. R. S. Devi, S. E. Koonin, and M. R. Strayer, in *Heavy Ion Science*, edited by D. A. Bromley (Plenum, New York, 1984).

²A. Vlasov, *J. Exp. Theor. Phys. (USSR)* **8**, 291 (1938).

³L. P. Kadanoff and G. Baym, *Quantum Statistical Mechanics* (Benjamin, New York, 1962).

⁴P. Danielewicz, *Ann. Phys.* **152**, 239 (1984); **152**, 305 (1984).

⁵L. W. Nordheim, *Proc. R. Soc. London, Ser. A* **119**, 689 (1928);

E. A. Uehling and G. E. Uhlenbeck, *Phys. Rev.* **43**, 552 (1933).

⁶H. S. Köhler and B. S. Nilsson, *Nucl. Phys.* **A477**, 318 (1988); H. S. Köhler, *Nucl. Phys.* **A494**, 281 (1989).

⁷H. S. Köhler, *J. Phys. (Paris)* **45**, C6-389 (1984); *Nucl. Phys.* **A440**, 16 (1985).

⁸W. Bauer, *Nucl. Phys.* **A471**, 604 (1987); G. F. Bertsch, H. Kruse, and S. Das Gupta, *Phys. Rev. C* **29**, 673 (1984).

⁹H. S. Köhler and B. S. Nilsson, *Nucl. Phys.* **A417**, 541 (1985).

¹⁰P. Danielewicz, *Phys. Lett.* **146B**, 168 (1984).